Plant Soil (2025) 516:725–746
https://doi.org/10.1007/s11104-025-07759-y

RESEARCH ARTICLE

Combining spring wheat genotypes with contrasting root architectures modifies plant–microbe interactions under different water regimes

Adrian Lattacher · Samuel Le Gall · Youri Rothfuss · Moritz Harings · Wolfgang Armbruster · Dagmar van Dusschoten · Daniel Pflugfelder · Samir Alahmad · Lee T. Hickey · Ellen Kandeler · Christian Poll

Received: 28 March 2025 / Accepted: 19 July 2025 / Published online: 30 August 2025

Abstract

Background and Aims Improving agricultural tolerance to climate change is crucial for food security. We investigated whether combining wheat genotypes with contrasting root architecture enhances plant performance under varying conditions. Specifically, we examined how these genotype mixtures affect nitrogen uptake, carbon release and root-microbe interactions compared to single-genotype plantings.

Methods We exposed monocultures and a mixture of shallow- and deep-rooting spring wheat (*Triticum aestivum* L.) genotypes separately to well-watered and water-deficit conditions in a column experiment. We determined plant and microbial biomass, major microbial groups, and β-glucosidase activity using soil zymography. Additionally, we followed carbon and nitrogen fluxes in the plant-soil-microorganism system by $^{13}CO_2$ labelling of the atmosphere and ^{15}N injection into top- and subsoil.

Results Combining wheat genotypes with contrasting root phenotypes influenced microbial activity and nutrient uptake depending on water availability. Under well-watered conditions, the mixture performed similarly to the respective monocultures. However, under water-deficit conditions, it exhibited complementary nutrient acquisition strategies where the deep-rooting genotype accessed deeper soil layers, while the shallow-rooting genotype relied more on topsoil nitrogen. This was accompanied by a reduced release of plant-derived carbon into the soil,

Responsible Editor: Peng Yu.

Supplementary Information The online version contains supplementary material available at https://doi.org/10.1007/s11104-025-07759-y.

A. Lattacher (✉) · E. Kandeler · C. Poll
Soil Biology Department, Institute of Soil Science and Land Evaluation, University of Hohenheim, 70599 Stuttgart, Germany
e-mail: adrian.lattacher@uni-hohenheim.de

S. Le Gall · Y. Rothfuss · M. Harings
Institute of Bio- and Geosciences, Agrosphere (IBG-3), Forschungszentrum Jülich, 52428 Jülich, Germany

W. Armbruster
Department of Food Chemistry and Analytical Chemistry, Institute of Food and Chemistry, University of Hohenheim, 70599 Stuttgart, Germany

D. van Dusschoten · D. Pflugfelder
Institute of Bio- and Geoscience, Plant Sciences (IBG-2), Forschungszentrum Jülich, 52428 Jülich, Germany

S. Alahmad · L. T. Hickey
Queensland Alliance for Agriculture and Food Innovation, The University of Queensland, St Lucia, QLD 4072, Australia

resulting in lower microbial abundance and reduced β-glucosidase activity compared to monocultures.
Conclusion Our results show that plants grown in a mixture performed similarly to monocultures under well-watered conditions while acquiring nutrients more efficiently under water-deficit conditions. This highlights the potential suitability of combining genotypes with contrasting root phenotypes under climate change. However, yield effects remained untested due to experimental constraints, warranting further investigation under field conditions.

Keywords Root phenotypes · Water deficit · Soil zymography · Rhizosphere · Intraspecific diversity

Introduction

High yielding cropping systems often lack tolerance to pests, diseases, and extreme climate events, all of which will increase in frequency and intensity under future climatic conditions (Østergård et al. 2009; Yuan et al. 2023). For this reason, new cultivation methods are currently being developed, including strategies to enhance crop diversity (Gaba et al. 2014; Isbell et al. 2017). While the benefits of interspecific diversity, the growing of different species in close proximity to each other, are well documented in both natural and agro-ecosystems, the effects of intraspecific diversity, the cultivation of different varieties of the same species in close proximity to each other, is less well studied (Bécu et al. 2024). Although different plant varieties exhibit less trait variability as compared to different plant species, their traits can still differ significantly (Cantarel et al. 2021). Wheat genotypes, for example, are known to differ in nitrogen use efficiency, plant performance under different fertiliser applications, and in their root traits (Colombo et al. 2022; Ivić et al. 2021). However, whether increasing intraspecific diversity in an agricultural system can influence the resilience of the system is not yet known.

The root system architectures of crops are crucial to their ability to take up water and nutrients from soil, directly impacting their growth, yield, and tolerance to environmental stresses (Langridge et al. 2021; Van der Bom et al. 2020). As climate change intensifies, leading to more frequent and severe droughts (Yuan et al. 2023), optimizing root systems for improved water and nutrient uptake has become a major focus in plant science (Paez-Garcia et al. 2015). Different root system architectures offer contrasting advantages in terms of water and nutrient uptake and transport. Shallow root systems (SRS) can quickly utilise the nutrients in topsoil, which are often more abundant there due to the higher fertilizer input and decomposition of organic matter (Nakhforoosh et al. 2021). Deep root systems (DRS), on the other hand, can access more mobile nutrients, especially nitrate, and water from deeper soil layers (Galindo-Castañeda et al. 2022). Harnessing the potential of combining wheat genotypes with contrasting root architecture of the same species could potentially improve drought resistance and nutrient utilisation efficiency leading to more resilient agro-ecosystems.

In addition to possible benefits in water uptake from different soil depths, the presence of different root systems can also influence the uptake, distribution, and availability of important soil resources such as nitrogen (N) and carbon (C) (Voss-Fels et al. 2018). Following nitrate fertilisation, for example, underdeveloped root systems cannot fully utilise the fertiliser, leading to its leaching and volatilisation (Dunbabin et al. 2003). A cultivation system with a wide range of rooting depths could help to capture fertilisers more efficiently and thus reduce leaching into the groundwater.

Combining plants with contrasting root architectures may also enhance plant–microbe interactions throughout the soil profile by modifying the distribution, abundance, and function of soil microorganisms, which are essential for nutrient mobilisation and supply to plants (Lattacher et al. 2025; Van der Bom et al. 2020). A combination of contrasting root architectures could improve microbe-root interactions within the entire soil profile through a more even distribution of rhizodeposits (i.e., exudates, cell debris, lysates). Rhizodeposits, especially root exudates, are known to promote microbial proliferation and activity in the rhizosphere, including stabilisation of C and mineralisation of nutrients (Keiluweit et al. 2015; Le Gall et al. 2024; Ma et al. 2022; Wen et al. 2022). Deep root systems, through their root exudates, can support microbial populations in deeper soil layers where microbial activity is typically lower due to limited organic C and oxygen availability (Beule et al. 2022). Shallow root systems, on the other hand, stimulate the proliferation

of microbial communities in the topsoil. This vertical stratification of microbial habitats can lead to a more diverse and resilient soil microbiome, capable of responding to environmental changes and supporting plant health and productivity under stress conditions (Galindo-Castañeda et al. 2024). In addition, the combined root systems could create a more favourable microenvironment for soil microorganisms under water-deficit conditions. Hydraulic lift provides an increased supply of water to the upper soil layers, which might be crucial for the survival and activity of soil microbes during drought periods (Liste and White 2008). The increased soil moisture not only supports microbial life but also promotes the microbial processes that are essential for nutrient cycling and decomposition of organic matter (Prieto et al. 2012). Consequently, improved water availability can promote microbially mediated nutrient turnover, increasing the availability of nutrients to plants.

In this study, we focussed on combining genotypes with contrasting root phenotypes of wheat (*Triticum aestivum* L.), since wheat is one of the most important staple foods worldwide, providing a significant proportion of the daily calorie intake for millions of people (Tadesse et al. 2019). Improving the tolerance and productivity of wheat through optimised root architecture is therefore of global importance (Ober et al. 2021). We were particularly interested in whether co-cropping of genotypes with contrasting root phenotypes has a beneficial impact on C and nutrient fluxes in the soil-microbiome-plant system under water-deficit conditions compared to using single genotypes in monoculture. We selected two experimental spring wheat lines with strongly contrasting seminal root angles. A wide root angle usually favours the formation of a shallow root system (SRS), while a narrow root angle leads to the formation of a deep root system (DRS) (Alahmad et al. 2019; Kang et al. 2024). The experimental spring wheat lines were grown in columns under two different water regimes, well-watered and water-deficit, in mono- and in mixed cultures. We studied the responses of C and N fluxes by isotopic labelling and how they affected the spatial distribution of microbial biomass and enzyme activity in soil. Le Gall et al. (in press) additionally investigated the root water uptake of the different genotypes under well-watered and water-deficit conditions in mono- and in mixed cultures in their study.

We hypothesized that a combination of genotypes with contrasting root architectures will increase microbial abundance and enzymatic activity throughout the soil profile compared to the monocultures, especially under water-deficit conditions, due to more efficient water use and more homogeneously distributed input of root exudates in top- and subsoil. The results of our study can help to develop effective strategies for managing soil fertility and crop tolerance under more extreme and changing climatic conditions.

Materials and methods

Experimental setup

Soil with a silt loam texture (22% clay, 66% silt, 12% sand) was collected from the upper 30 cm of a Haplic Luvisol (Cai et al. 2016) in an agricultural field located in Selhausen, Germany (50°52′07.8″ N, 6°26′59.7″ E) in November 2020 (Weihermüller et al. 2007). The soil was homogenized, sieved to 2 mm, and air-dried. Columns with an internal diameter of 11 cm and a height of 80 cm (7.6 L volume) were filled with 10.64 kg air-dried soil and compacted using a vibrating plate (Haver EML 450 Digital Plus N, Haver & Boecker, Oelde, Germany) to achieve dry bulk density of 1.4 g cm^{-3}, which is representative of field conditions. Bulk density was kept homogeneous throughout the soil profile to limit variations that could affect root development and water infiltration. The soil of all columns was then saturated with water from the bottom of the column via a porous plate, simulating a moist spring, to enable similar conditions for germination and initial plant growth. Once saturation was reached, soil columns were left to stabilize at field capacity for two weeks. After this period, water was applied from the surface according to the"WW" and “WD"treatments, simulating rainfall events. For this column experiment, two experimental spring wheat (*Triticum aestivum* L.) lines, UQR012 (shallow root system: SRS) and UQR015 (deep root system: DRS), with strongly contrasting seminal root angles (Rambla et al. 2022), were used. UQR012 exhibited a wider seminal root angle of approximately 110°, which leads to the formation of a shallower root system, whereas UQR015 displays a narrower angle of about 66°, resulting in a deeper root system (Rambla

et al. 2022). The genotypes were developed by backcrossing a donor source for narrow root angle to the high-yielding spring wheat cultivar Borlaug100. The plants were grown in mono- (SRS or DRS) and mixed cultures (MIX) in a climate chamber under controlled conditions. Four seeds were sown per column, and after emergence, the two strongest seedlings were selected and retained. Each monoculture column contained two plants of the same genotype (either SRS or DRS), while each mixed culture column contained one plant of each genotype (SRS and DRS). Air temperature was set to 20 ± 0.22 °C, relative humidity was set to 50.0 ± 2%. The light intensity followed a sinusoidal 24-h cycle from 0 µmol m^{-2} s^{-1} at"night"(from 8 pm to 6 am) to 1200 µmol m^{-2} s^{-1} at"midday"(1 pm). Watering regimes were adjusted to vary in intensity, targeting a soil matric potential (pF) of 2.0–3.0 for the"well-watered"(WW) treatment and a pF of 3.5–4.5 for the"water-deficit"(WD) treatment. The amount of water added over the 6-week experimental period corresponded to approximately 137 mm and 21 mm of cumulative precipitation for the WW and WD treatments, respectively. This resulted in the following treatments: WW-SRS, WW-DRS, WW-MIX, WD-SRS, WD-DRS and WD-MIX. Each treatment was replicated three times in three separate runs due to spatial limitation in the climate chamber, i.e., each run consisted of one replicate of each treatment. Growing conditions and treatments were kept identical across all runs, while the spatial positions of the treatments in the climate chamber were randomized within each run to avoid positional bias and ensure that treatment effects were not confounded by potential microenvironmental differences within the chamber (Table S1). For the N, C and microbial analyses described in this study, "PVC soil columns" were used, while Le Gall et al. (in press) used "acrylic soil columns" to determine the root water uptake in their study (Fig. 1). At the three-leaf stage, mineral fertiliser (calcium ammonium nitrate) equivalent to 60 kg N ha^{-1} was applied to each soil column. On day 39 after sowing, the subsoil (75 cm) was labelled with a 5 atom% ^{15}N-NH_4NO_3 solution, equivalent to 10 kg N ha^{-1}. It was injected using a syringe through a silicone-covered port on the side of the column to investigate the flow of N from the subsoil into the plant. Forty-eight hours after labelling, small parts of the youngest fully developed leaves of each plant were sampled. Immediately after the first leaf sampling, we labelled the topsoil with a more highly labelled solution of 20 atom% ^{15}N-NH_4NO_3, equivalent to 10 kg N ha^{-1}, at a soil depth of 5 cm, and 48 h later parts of the youngest fully developed leaves were sampled again. At the same time as the ^{15}N labelling of the topsoil, plants were pulse-labelled for 4 h with ^{13}C-CO_2 using an airtight chamber to track the flow of C from the plants into the soil and soil microorganisms. For the fumigation of the plants with ^{13}C-CO_2, 20 atom% ^{13}C-sodium bicarbonate was used, which was released stepwise with 8.5% phosphoric acid over a period of 4 h. For this purpose, the CO_2 uptake of the plants was determined one day before labelling using an isotope-ratio mass spectrometer (Thermo Fisher Scientific Inc., Waltham, MA, USA). Based on the air volume of the chamber, the required amount and the interval of phosphoric acid additions was calculated to release 400 ppm CO_2 from the sodium bicarbonate at a time. According to the calculations, the CO_2 target concentration during pulse labelling was between 400 and 800 ppm.

Fig. 1 Experimental setup of the columns in the climate chamber (**a**) showing the PVC columns (red) used for carbon, nitrogen and microbial analysis and the MRI root scans in this experiment and the acrylic columns (blue) which were used to determine root water uptake by Le Gall et al. (in press). Airtight chamber (**b**) used for $^{13}CO_2$ pulse labelling of the plants

At the 6th week of plant growth, the root systems of the plants in the PVC columns were analysed non-destructively using a 4.7 T magnetic resonance imaging (MRI) magnet (Magnex, Oxford, UK) and a MR Solutions console (MR solutions, Guildford, UK). Roots with a diameter > ~350 µm were visible, which was sufficient to visualise the seminal and basal root structure of the plants. Root length was determined with a vertical resolution of 2.5 cm by processing the MRI images with the NMRooting software according to Van Dusschoten et al. (2016). The MRI signal intensity, which is proportional to the water content of the roots, was used to estimate the root biomass. Usually, a calibration to the fresh weight of the roots can be made; however, since the soil and columns used in this study had not been previously analysed with this device, such a calibration was not available. Therefore, root biomass is expressed in arbitrary units (a.u.) reflecting proportionality to the fresh weight of the roots with an unknown proportionality constant. Roots were segmented using a convolutional neural network developed with nnU-Net (Isensee et al. 2021). In contrast to Le Gall et al. (in press), the MRI root scan analysis in this study was limited to three replicates instead of six, as subsequent C, N, and microbial measurements were only conducted on these three replicates.

Forty-three days after sowing, when the plants had reached ear emergence from the boot (equivalent to Z51-59 on the Zadoc scale), the aboveground plant biomass was removed. After finalization of each run, the soil was extracted from the columns and sliced into 10 cm segments of which we sampled selected topsoil (0–10, 10–20 and 20–30 cm) and subsoil (50–60, and 60–70 cm) layers which were first used for none-destructive analysis (soil zymography) followed by destructive soil analyses. The 70–80 cm segment was excluded from further analysis to avoid potential bias of results from root accumulation at the bottom of the columns. To create the planar surfaces required for soil zymography, the 10 cm thick soil cores were cut horizontally in half with a sharp knife (Lattacher et al. 2025). Following non-destructive analysis, the roots were removed from the segments. Separation of soil from the roots was done by gently shaking the roots with the adhering soil for 1 min in a plastic container (Gobran and Clegg 1996). The soil collected during this step was combined with the soil from the respective soil segment, which was then sieved to 2 mm for further analysis. The remaining soil was afterwards carefully washed off the roots using water to allow for subsequent root measurements. Plants were further separated into roots, stems and leaves to determine the biomass and isotopic signal of the different plant organs. In comparison to the previous sampling to measure uptake of ^{15}N in the youngest leaves of the plant, a pooled sample of all leaves from one plant was produced at the end of the incubation. All samples were frozen at −20 °C until analysis.

^{13}C and ^{15}N in plants and soil

To determine soil water content, dry plant biomass and the $\delta^{13}C$ and $\delta^{15}N$ in soil and different plant organs (roots, stem, and leaves) samples were dried at 60 °C for 72 h, weighed, and subsequently ground. Subsamples of 20 mg (±2 mg) for the soil and 3 mg (±0.5 mg) for the plant material were then weighed into tin capsules and analysed according to Preusser et al. (2021) using an elemental analyser (Euro 3000, Euro Vector, Italy) coupled with an isotope ratio mass spectrometer (Delta Plus XP, Thermo Finnigan, Germany).

Soil zymography and imaging procedure

Soil zymography was performed on the top of the plane surface of the freshly extracted top- and subsoil segments using the fluorogenic substrate 4-methylumbelliferone-β-D-glucopyranoside (Sigma Aldrich, Germany) to evaluate the spatial distribution of β-glucosidase (BG) activity according to Razavi et al. (2016). The substrate, dissolved in dimethyl sulfoxide (Sigma Aldrich, Germany), was diluted to 5 mM using deionized and autoclaved water. A 0.2 µm pore size polyamide membrane filter (Sartorius, India) was soaked with the substrate solution and placed directly on the soil surface, following slight moistening of the soil to enhance substrate diffusion (Guber et al. 2021). After 1 h dark incubation at 20 °C, the filter was removed and exposed to UV light (365 nm) using the BioDOC Analyzer (Biometra, Germany). Images were captured (RICOH TV-200 M 8–48 mm) with an exposure time of 75 ms and an enhancement of 5 using BioDocAnalyze software. Membrane snippets (3×1 cm^2) were soaked in solutions with different

concentrations of 4-methylumbelliferone (MUF) (0, 0.05, 0.1, 0.15, 0.2 and 0.3 mM) for calibration. The calibration function was calculated by relating the measured fluorescence to the volume of MUF solution absorbed by the polyamide membrane and its size (Razavi et al. 2016). ImageJ software (Abramoff et al. 2004) with the Fiji package (version 2.1.0) was used for image processing. Zymograms were converted to 8-bit greyscale images and background fluorescence of the filters soaked with MUF substrate solution was subtracted. The grey values were converted to MUF per membrane area (pM mm^{-2}) using the calibration function ($R^2 = 0.99$). A small piece of paper of known size was used to set the scale using the "Set Scale" function of ImageJ. Average enzyme activity was calculated using histogram data from the calibrated and background-corrected zymograms. Based on other studies, enzymatic hotspots were defined as grey value > 150% of the mean grey value of all images (Heitkötter and Marschner 2018; Hao et al. 2022; Lattacher et al. 2025) which, in this study, was equivalent to an enzymatic activity equal to or higher than 26 pM mm^{-2} h^{-1}. The areas corresponding to these hotspots were quantified as a percentage of the overall soil surface area.

The gradient of BG activity from the root centre towards the surrounding soil was determined using the "Plot Profile" function of ImageJ, spanning a distance of 0 to 26 mm from the root centre. A line width of 5 pixels (equivalent to 620 µm) was used on 4–9 roots for each genotype, water regime, and depth. To determine the activity of BG from the root centre towards the surrounding soil, we selected the area on the roots with the highest enzymatic activity. The BG activity gradient was then plotted against the distance. The decrease in enzyme activity E(x) from the root centre towards the surrounding soil was described using an exponential decay function (Lattacher et al. 2025):

$$E(x) = E_0 \cdot exp(-kx) + E_{bulk} \quad (1)$$

where E_0 is the initial enzyme activity (pM mm^{-2} h^{-1}) close to the root centre, x is the distance to the root centre (mm), k is a first-order rate coefficient (1 mm^{-1}) of enzyme activity decrease and E_{bulk} represents the mean enzyme activity (pM mm^{-2} h^{-1}) in bulk soil.

Soil microbial carbon and plant-derived ^{13}C incorporation

Microbial carbon (C_{mic}) content was determined using the chloroform fumigation extraction method described by Vance et al. (1987). Two subsamples of 1 g soil each were weighed from all samples of all runs. One subsample was fumigated in a desiccator with ethanol-free chloroform for 24 h to release C_{mic}. Both the fumigated and non-fumigated subsamples were then extracted with 10 ml of a 0.025 M K_2SO_4 solution, shaken at 200 rpm for 30 min and centrifuged at 4400 g for 30 min. After centrifugation, supernatant was transferred to a scintillation vial using a 5 ml pipette equipped with a 20 µm filter at the tip to prevent inclusion of organic particles. Supernatants were frozen at −20 °C until analysis. Organic carbon (C_{org}) in the supernatants was quantified using the TOC-TNb Multi N/C 2100S analyser (Analytik Jena, Germany). C content of the microbial biomass (µg C g^{-1}) was calculated by subtracting the C content of the non-fumigated extracts from that of the fumigated extracts, using the kEC factor of 0.45 according to Joergensen (1996) to correct for the extractable fraction of total C bound in the microbial biomass. In addition, the non-fumigated samples were used to determine extractable organic C (EOC).

To determine the $\delta^{13}C$ in C_{mic} ($\delta^{13}C_{mic}$), 8 ml of both fumigated and unfumigated extracts were evaporated in a rotary evaporator (RVC 2–25, Christ, Germany). After evaporation, 20 mg (± 2 mg) of the residues were weighed into tin capsules and isotopic composition was measured using an elemental analyser (Euro EA 3000, Euro Vector, Italy), coupled to an isotope ratio mass spectrometer (Delta Plus XP, Thermo Finnigan MAT, Germany). The $\delta^{13}C_{mic}$ was calculated according to Marhan et al. (2010) using the following equation:

$$\delta^{13}C_{mic} = \frac{\delta_f \times C_f - \delta_{nf} \times C_{nf}}{C_f - C_{nf}} \quad (2)$$

where C_f and C_{nf} represent the extractable organic C content of the fumigated and non-fumigated samples, and δ_f and δ_{nf} are the corresponding $\delta^{13}C$ values.

Phospholipid and neutral fatty acids and plant-derived ^{13}C incorporation

The major microbial groups in soil were quantified by extracting phospholipid and neutral fatty acids (PLFAs, NLFAs) from microbial cell membranes. Extraction, fractionation, and quantification of the lipids followed the methodologies outlined by Bardgett et al. (1996), which were adapted from the procedures established by Frostegård et al. (1991) and Bligh and Dyer (1959). In brief, 4 g soil was mixed with Bligh & Dyer solution (with a ratio of chloroform: methanol: citrate buffer of 1:2:0.8) to extract the lipids. Next, a solid phase extraction was performed using extraction columns (Bond Elut, Agilent Technologies, USA) to separate NLFAs from PLFAs. Subsequently, the PLFAs and NLFAs were transformed into fatty acid methyl esters (FAMEs) by alkaline methanolysis using the method described by Kramer and Gleixner (2008). An internal standard of FAME C24:1 (Sigma-Aldrich, St. Louis, MO, USA) was added to the samples prior to methanolysis. In accordance with Kandeler (2015), the fatty acids i15:0, a15:0, i16:0 and i17:0 were selected as representative of gram-positive bacteria ($PLFA_{GP}$) while cy17:0 and cy19:0 were selected to represent the gram-negative bacteria ($PLFA_{GN}$). The fatty acid 18:2ω6,9 was used as an indicator for fungi ($PLFA_{fun}$) (Federle 1986). In addition, the NLFA 16:1ω5 was used as a biomarker for arbuscular mycorrhizal fungi ($NLFA_{AMF}$) (Olsson et al. 1998). Extracted FAMEs were analysed using an Agilent 8860 gas chromatograph with a flame ionization detector (FID) and a 5977B mass selective detector (MSD) (Agilent, USA). The FID was used for quantification, the MSD for FAME identification. Calibration was performed using a bacterial methyl ester mixture (Sigma-Aldrich, USA) and individual standard FAMEs. The $\delta^{13}C$ values of the PLFA and NLFA samples were measured using an HP 6890 gas chromatograph (Agilent Inc., USA) equipped with a combustion III interface (Thermo Finnigan, USA) connected to a Delta Plus XP mass spectrometer via a Conflo IV Interface (bboth Thermo Finnigan MAT Germany). The samples (analytes) were separated using an HP-5 GC column (Agilent Inc., USA) with a helium flow of 1.5 ml min^{-1}. The $\delta^{13}C$ values of all FAMEs were corrected to account for the addition of a methyl group.

Statistical analyses

Statistical analyses were performed in R (Version 4.2.0; R Core Team 2020). The Shapiro–Wilk and Levene tests from the car package (Fox and Weisberg 2019) were used to test for normality and homoscedasticity of variance, respectively. The significance of differences ($\alpha < 0.05$) was assessed with a linear mixed-effects model using the lme function from the nlme package (Pinheiro and Bates 2000). Genotype, depth, and water regime were considered as fixed effects, while columns and runs were treated as random effects (see Supplementary).

To model the enzyme gradient within the rhizosphere, a non-linear mixed-effects model was fitted to BG activity with increasing distance from the root centre. This nonlinear mixed-effects model was simplified based on the significance of factors and interactions to identify the most important components of the model and to avoid overfitting. The significance of the differences was then tested by performing an ANOVA with the simplified model.

Results

Aboveground plant biomass

The DRS showed a non-significant trend towards a higher aboveground biomass compared to the SRS across all treatments (Fig. 2). While the monocultures of DRS and SRS were similar in biomass across the different water regimes, the mixtures showed contrasting responses of the two genotypes. A greater variability in aboveground plant biomass was observed within the mixture, especially for SRS and DRS under water-deficit conditions, as well as for SRS within the mixture under well-watered conditions. The DRS in the mixture was 44% lower in biomass under water-deficit conditions than under well-watered conditions, while the SRS in the mixture had a 30% increase in biomass under water-deficit conditions.

While $\delta^{13}C$ values in leaves and stems were not significantly different between genotypes and water

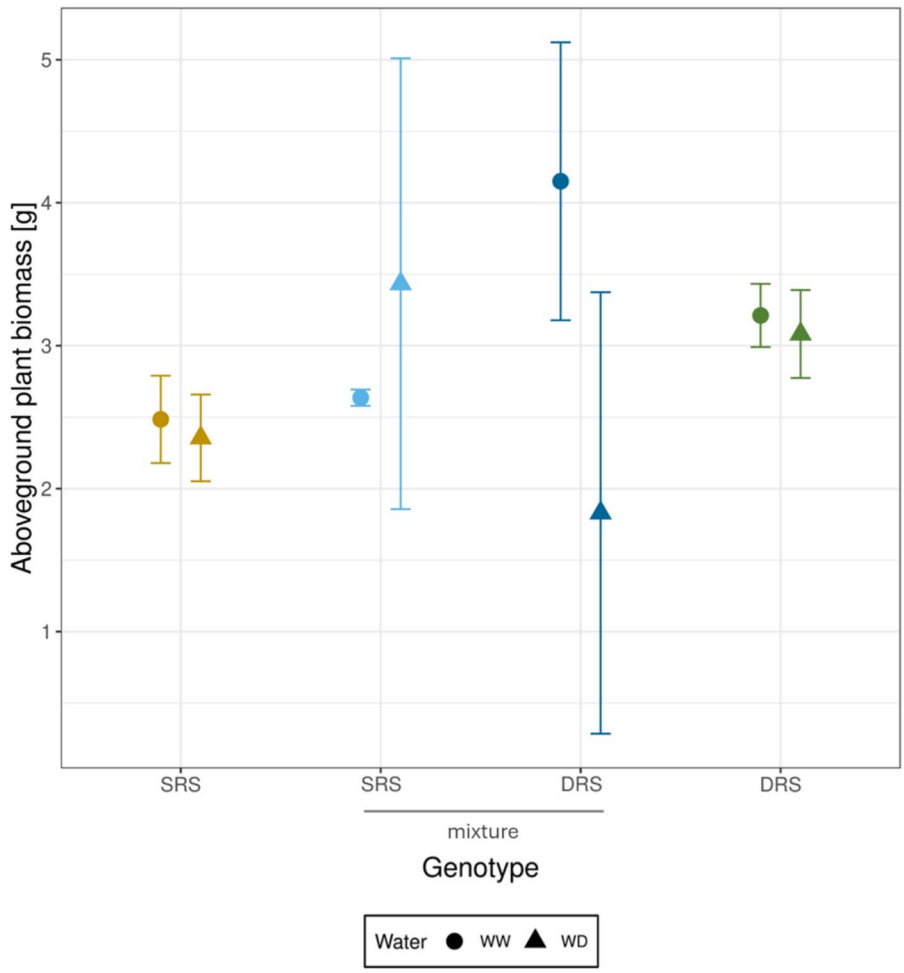

Fig. 2 Mean dry aboveground plant biomass in g per plant for the genotype with the shallow root system (SRS) in monoculture (yellow) and mixture (light blue) and for the genotype with the deep root system (DRS) in monoculture (green) and mixture (dark blue). Data represent means ± standard deviation of three replicates, conducted across three runs. Circles represent the mean above ground dry plant biomass per plant under well-watered conditions (WW) while triangles represent the mean plant biomass under water-deficit conditions (WD)

regimes (Fig. S1a), the $\delta^{15}N$ signal was lower in the DRS, both in monoculture and mixture compared to the SRS in the pooled leaves (genotype, $p < 0.05$) and stem (genotype, $p < 0.05$; Fig. S1b). Data for the pooled leaves and stems were taken after the ^{13}C-pulse labelling and, therefore, integrated both ^{15}N-labelling events.

The ^{15}N data of the youngest leaves made it possible to separate N uptake from two different depths. In the youngest leaves no significant differences in the $\delta^{15}N$ signal between genotypes and water regimes were found two days after labelling the subsoil (Fig. 3). However, a non-significant increased $\delta^{15}N$ signal was detected under water-deficit conditions in the youngest leaves for the DRS in mixture, with a $\delta^{15}N$ of 381‰ compared to the SRS in mixture (93‰) and the DRS and SRS in the monocultures (135‰ and 119‰). After topsoil labelling the $\delta^{15}N$ signal in the youngest leaves of DRS in both monoculture and mixture tended to be lower compared to the respective SRS while no differences between water-deficit and well-watered conditions were detected for either genotype.

Belowground plant biomass

Depth profiles of dry root biomass and calculated fresh root biomass from the magnetic resonance imaging (MRI) data were generally similar across genotypes and water regimes (Figs. 4a and 5). However, the MRI data indicated a significantly higher root biomass under well-watered conditions for the SRS in the topsoil (from 3–15 cm; genotype, $p < 0.05$) and the DRS in the subsoil (70–80 cm; genotype, $p < 0.05$) compared to the MIX in both soil depths and the respective monocultures (DRS

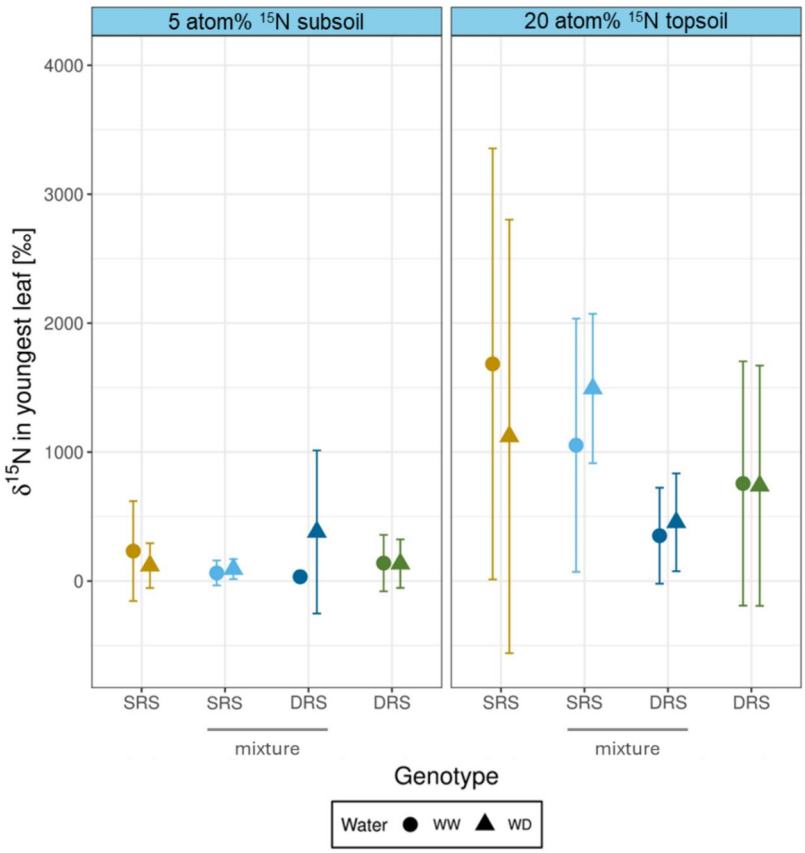

Fig. 3 $\delta^{15}N$ signal in youngest fully developed leaf for the genotype with the shallow root system (SRS) in monoculture (yellow) and mixture (light blue) and for the genotype with the deep root system (DRS) in monoculture (green) and mixture (dark blue) after subsoil labelling with 5 atom% ^{15}N-NH_4NO_3 and topsoil labelling with 20 atom%.^{15}N-NH_4NO_3. Data represent means ± standard deviation of three replicates, conducted across three runs. Circles represent the mean values under well-watered conditions (WW) while triangles represent the mean values under water-deficit conditions (WD)

and SRS). The $\delta^{13}C$ signal measured in the root biomass was significantly higher under well-watered than water-deficit conditions (water, $p < 0.05$; Fig. 4b) and in the subsoil (60–70 cm) compared to the upper soil layers, independent of the water regime and genotype (depth, $p < 0.01$). At 60–70 cm soil depth, the MIX and DRS tended towards a higher $\delta^{13}C$ signal in the roots compared to the SRS for both wate r regimes.

Soil water and $\delta^{13}C$

The gravimetric water content in soil was significantly higher under well-watered than water-deficit conditions (water, $p < 0.01$; Fig. S2). Although the $\delta^{13}C$ values in soil did not differ significantly, the WD-MIX tended towards a low $\delta^{13}C$ signal compared to all other treatments. The $\delta^{13}C$ of WD-MIX was close to the ambient signal in unlabelled soil (−27‰) except at a soil depth of 60–70 cm where an increased $\delta^{13}C$ signal was found (Fig. 6).

Microbial biomass and community structure

While C_{mic} was not significantly different between genotypes and water regimes (Fig. S3a), the $\delta^{13}C$ signal in C_{mic} tended towards a higher incorporation of plant-derived ^{13}C into microbial biomass in the WW-MIX (mean $\delta^{13}C_{mic} = +8.90‰$) compared to the WD-MIX (mean $\delta^{13}C_{mic} = -20.9‰$) (Fig. S3b).

The abundances of $PLFA_{GP}$, $PLFA_{GN}$ and $PLFA_{fun}$ showed similar patterns (Fig. 7a, 7b, 7c): under water-deficit conditions, lower abundance of these microbial PLFAs in MIX compared to the monocultures was observed. In contrast, the opposite effect was observed under well-watered conditions for $PLFA_{GN}$ and $PLFA_{GP}$. The abundance of $PLFA_{GN}$ tended to be lower in the MIX under water-deficit compared to well-watered conditions (genotype × water,

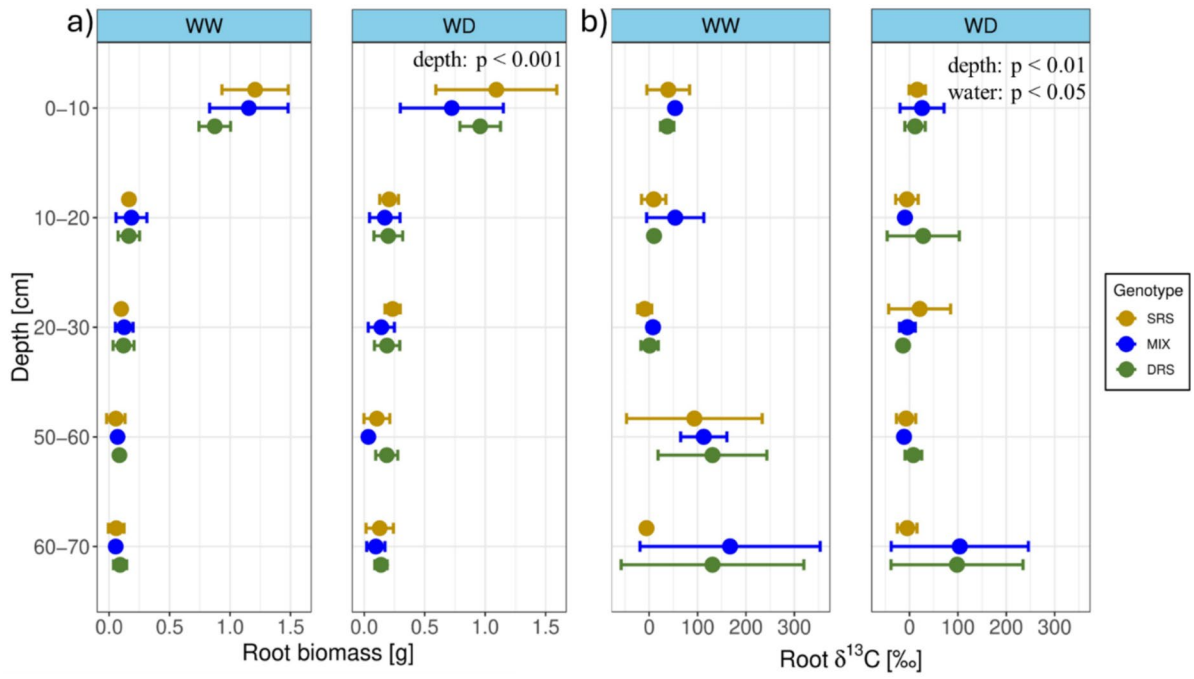

Fig. 4 Dry root biomass (**a**) and $\delta^{13}C$ signal in roots (**b**) in various soil depths for the deep root system (DRS) (green), shallow root system (SRS) (yellow) and the mixture (MIX) (blue) under well-watered (WW) and water-deficit (WD) conditions. Data represent means ± standard deviation of three replicates, conducted across three runs

$p = 0.07$). This effect was not observed for $PLFA_{GP}$ and $PLFA_{fun}$, but these groups displayed a similar, albeit non-significant, pattern. The $PLFA_{GP}$ exhibited a weak response to the water regime (depth × water, $p = 0.08$), with lower abundance under water-deficit than well-watered conditions in the upper soil layers, which was particularly pronounced for MIX.

The $\delta^{13}C$ signal in the PLFAs was strongly affected by the water regime in soil. The $\delta^{13}C$ signal in $PLFA_{GP}$ (Fig. 8a), $PLFA_{GN}$ (Fig. 8b) and $PLFA_{fun}$ (Fig. 8c) in the DRS was higher under water-deficit than well-watered conditions, which was especially pronounced at 60–70 cm (genotype × water: $PLFA_{GP}$: $p < 0.05$; $PLFA_{GN}$: $p = 0.06$; genotype × water × depth: $PLFA_{fun}$: $p < 0.05$). The opposite was true in SRS, particularly for $PLFA_{GN}$. It was also observed that the fungal PLFAs had, especially in the subsoil, a much higher $\delta^{13}C$ signal compared to the bacterial PLFAs.

The abundance of $NLFA_{AMF}$ were not significantly different between the genotypes and water regimes but tended towards lower abundance in the mixture compared to the monocultures under water-deficit conditions (Fig. 7d) especially in topsoil. Additionally, in the monocultures, a tendency towards higher abundance of $NLFA_{AMF}$ in the SRS in the topsoil and the DRS in the deeper layers was observed (genotype × depth, $p = 0.07$). While under well-watered conditions the highest abundance of $NLFA_{AMF}$ was found in 0–10 cm soil depth for all cultures, under water-deficit conditions a different pattern was observed. Here the DRS and MIX showed the highest $NLFA_{AMF}$ abundance at 10–20 cm soil depth, while the SRS showed the highest abundance at 0–10 cm soil depth.

The $\delta^{13}C$ value in the $NLFA_{AMF}$ did not differ significantly between genotypes and water regimes (Fig. 8d). WD-DRS, compared to the other treatments, did not have the highest $\delta^{13}C$ signal at 0–10 cm, but at 20–30 cm soil depth. In comparison to the bacterial PLFAs, the $\delta^{13}C$ signal in $NLFA_{AMF}$ notably increased, particularly at the 0–10 cm and 20–30 cm soil depths. However, at 60–70 cm soil depth, the saprotrophic $PLFA_{fun}$ had a higher $\delta^{13}C$ signal compared to $NLFA_{AMF}$.

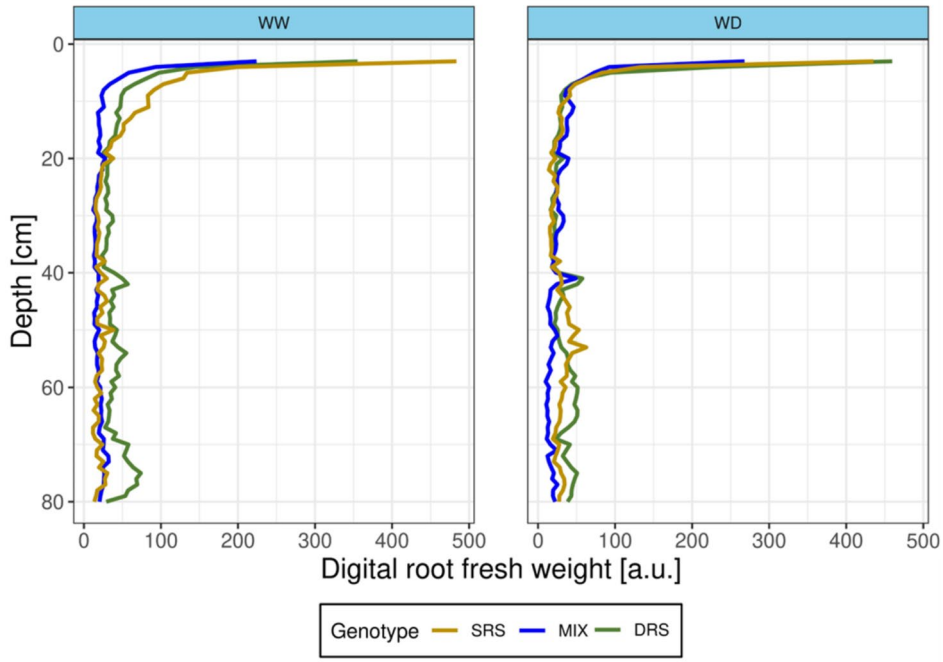

Fig. 5 Profile of the MRI-determined digital root fresh weight for the deep root system (DRS) (green), shallow root system (SRS) (yellow) and mixture (MIX) (blue) from 3 to 80 cm under well-watered (WW) and water-deficit (WD) conditions. Data represent means of 3 replicates conducted across three runs

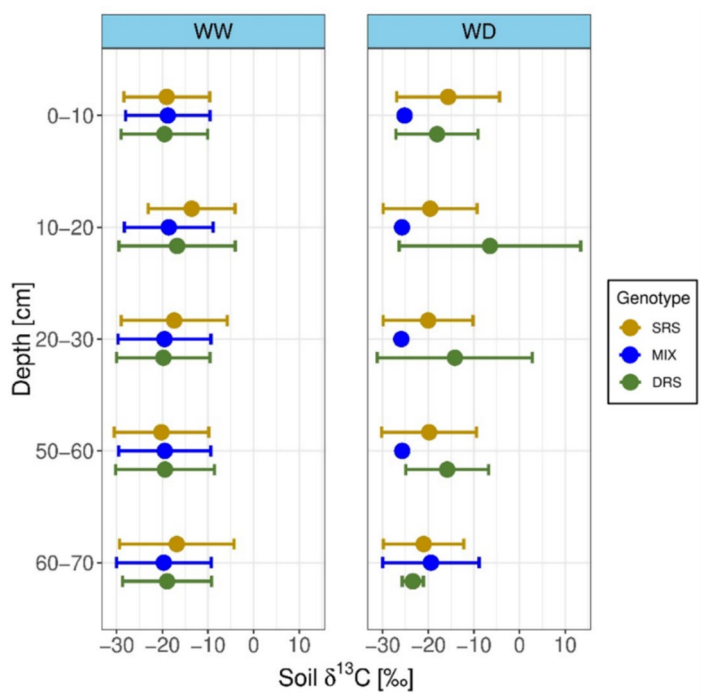

Fig. 6 $\delta^{13}C$ signal in soil at various soil depths for the deep root system (DRS) (green), shallow root system (SRS) (yellow) and the mixture (MIX) (blue) under well-watered (WW) and water-deficit (WD) conditions. Data represent means ± standard deviation of three replicates, conducted across three runs

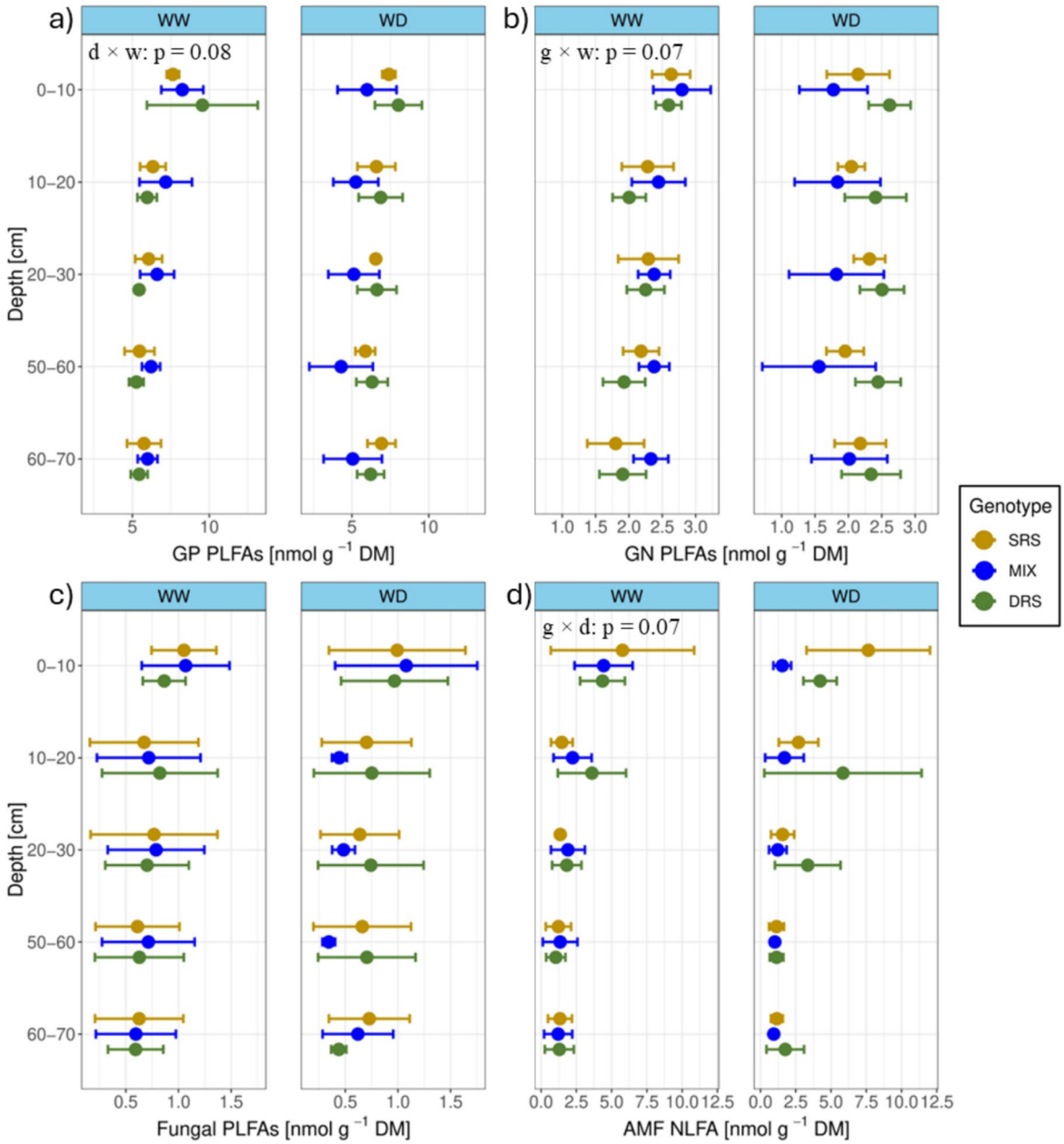

Fig. 7 Abundance of gram-positive bacterial PLFAs (**a**), gram-negative bacterial PLFAs (**b**), fungal PLFAs (**c**) and arbuscular mycorrhizal fungal NLFAs (**d**) at various soil depths for the deep root system (DRS) (green), shallow root system (SRS) (yellow) and the mixture (MIX) (blue) under well-watered (WW) and water-deficit (WD) conditions. Data represent means ± standard deviation of three replicates, conducted across three runs. Interaction effects of genotype (g), depth (d), and water regime (w) are indicated in the panels

β-glucosidase activity

Under water-deficit conditions, the mixture consistently exhibited the lowest BG activity and hotspot areas compared to both the monocultures and the mixture under well-watered conditions. However, these differences were not statistically significant (Fig. 9). While the monocultures (SRS and DRS)

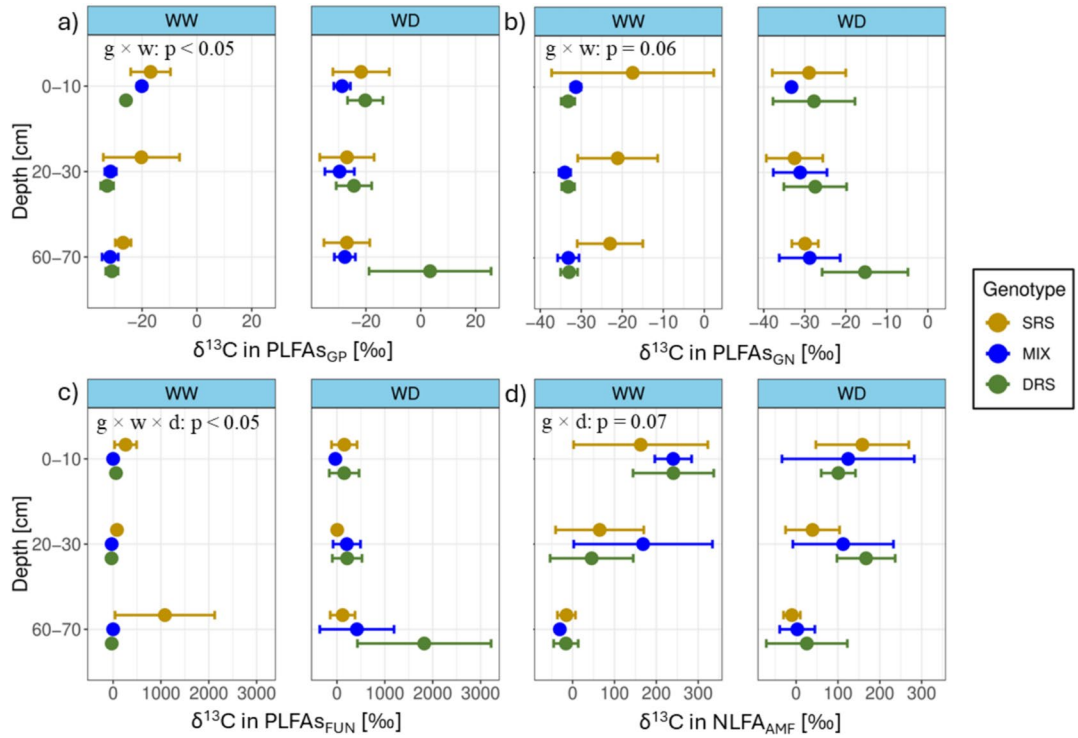

Fig. 8 $\delta^{13}C$ signal in gram-positive bacterial PLFAs (a), gram-negative bacterial PLFAs (b), fungal PLFAs and arbuscular mycorrhizal fungal NLFAs at various soil depths for the deep root system (DRS) (green), shallow root system (SRS) (yellow) and the mixture (MIX) (blue) under well-watered (WW) and water-deficit (WD) conditions. Data represent means ± standard deviation of three replicates, conducted across three runs. Interaction effects of genotype (g), depth (d), and water regime (w) are indicated in the panels

showed very similar gradients in BG activity around the roots within the same soil depth irrespective of the water regime, root BG gradients in MIX treatments were significantly affected by the water regime (Fig. 10). WD-MIX was significantly lower in BG activity near the root centre (E_0) in 0–60 cm soil depth (genotype × depth × water, $p < 0.05$) and tended towards lower BG activity in the bulk soil averaged across the entire soil profile (E_{bulk}) (genotype × water, $p = 0.07$) than WW-MIX, as shown by the lower BG activity as distance from the root centre increased.

Discussion

Our study investigated the effect of combining genotypes with contrasting root phenotypes of wheat under well-watered and water-deficit conditions on microbial community and activity at various soil depths. We additionally used stable isotopes to follow C and N fluxes in the plant-soil system. We primarily found that, in contrast to our hypothesis, a combination of genotypes with contrasting root phenotypes tended towards lower root exudation, microbial abundance, and enzymatic activity under water-deficit conditions compared to the monocultures at most soil depths. This trend was not visible when the combination of genotypes with contrasting root phenotypes was grown under well-watered conditions, indicating a strong impact of the water regime on the plant-root interactions of such combined plant systems. The genotypes differed in their major N uptake zones with the DRS in the mixture targeting deeper soil layers under water-deficit conditions and the SRS relying more on topsoil N.

Above- and below-ground plant biomass

One of the ideas behind combining genotypes with contrasting root phenotypes in one field is to improve

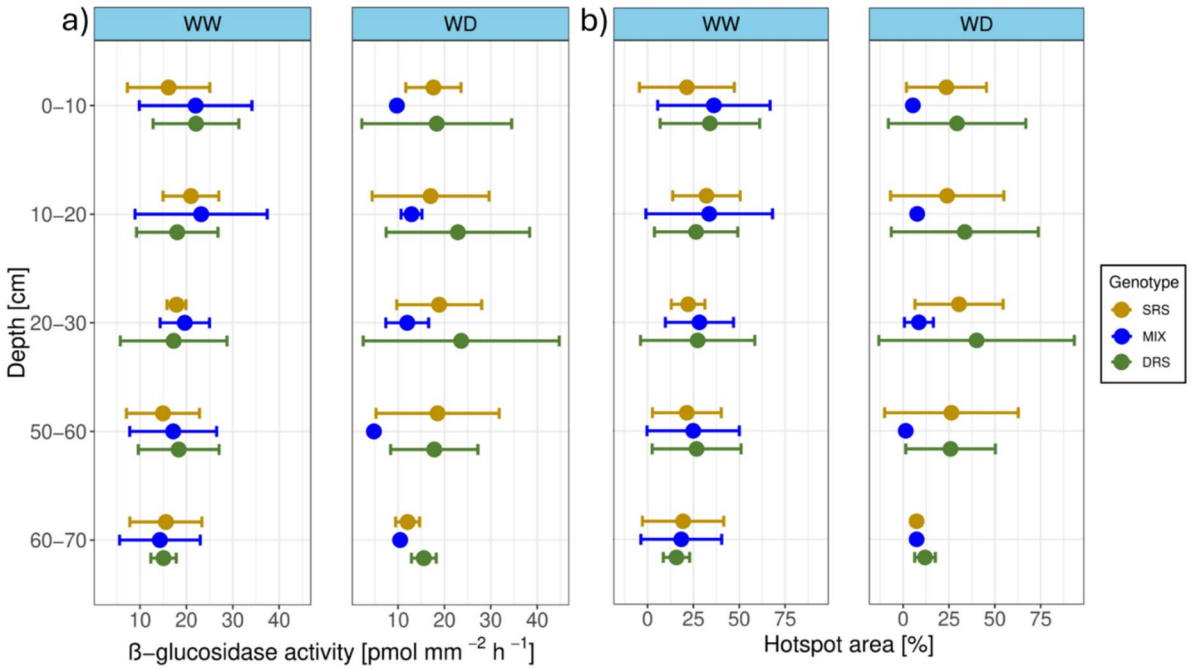

Fig. 9 β-glucosidase activity (**a**) and hotspot areas (**b**) at various soil depths for the deep root system (DRS) (green), shallow root system (SRS) (yellow) and the mixture (MIX) (blue) under well-watered (WW) and water-deficit (WD) conditions. Data represent means ± standard deviation of three replicates, conducted across three runs

the stability of plant production under water limitation conditions while having no negative effects under optimal plant growth conditions. In our experiment total aboveground biomass per column did not differ between mixtures and monocultures under either well-watered or water-deficit conditions. However, individual plant biomass within mixtures was highly dependent on the prevailing water regime. A likely explanation for this genotype-specific response lies in nitrogen fertilization during the three-leaf stage. Under water deficiency, nitrate mobility may have been severely limited (Joseph et al. 2021), causing most of the nitrate to remain in the topsoil, where it was more accessible to the SRS in the mixture, promoting its growth. Under well-watered conditions, nitrate likely leached to the subsoil (Jamali et al. 2015), favouring uptake by the DRS and enhancing its growth. In mixtures, reduced competition for nutrients might have allowed individual plants to grow more than in monocultures, where both plants accessed similar soil layers. In monocultures, where both plants shared similar rooting strategies and occupied the same soil layers, nitrogen availability was likely more evenly distributed among individuals, which could explain the more uniform biomass outcomes. Absence of differences in aboveground biomass between genotypes in monoculture under different water regimes further suggests that the applied water-deficit treatment did not induce water stress in a way which negatively impacted overall biomass production. The observed larger variability in aboveground biomass in the mixtures, especially for SRS under water-deficit conditions and for DRS under both water regimes, can be explained by individual differences in response to localized environmental conditions. Lichstein et al. (2007) showed that intraspecific variation can arise from both properties of individuals and environmentally induced factors that act independently among individuals. In our system, the combination of genotypes with contrasting root phenotypes leads to different access to nutrients and water among individual plants, which could explain the observed variability. Thus, the mixture's flexibility in resource acquisition may come at the cost of greater variability at the individual plant level which might become beneficial in the face of increasing extreme weather events.

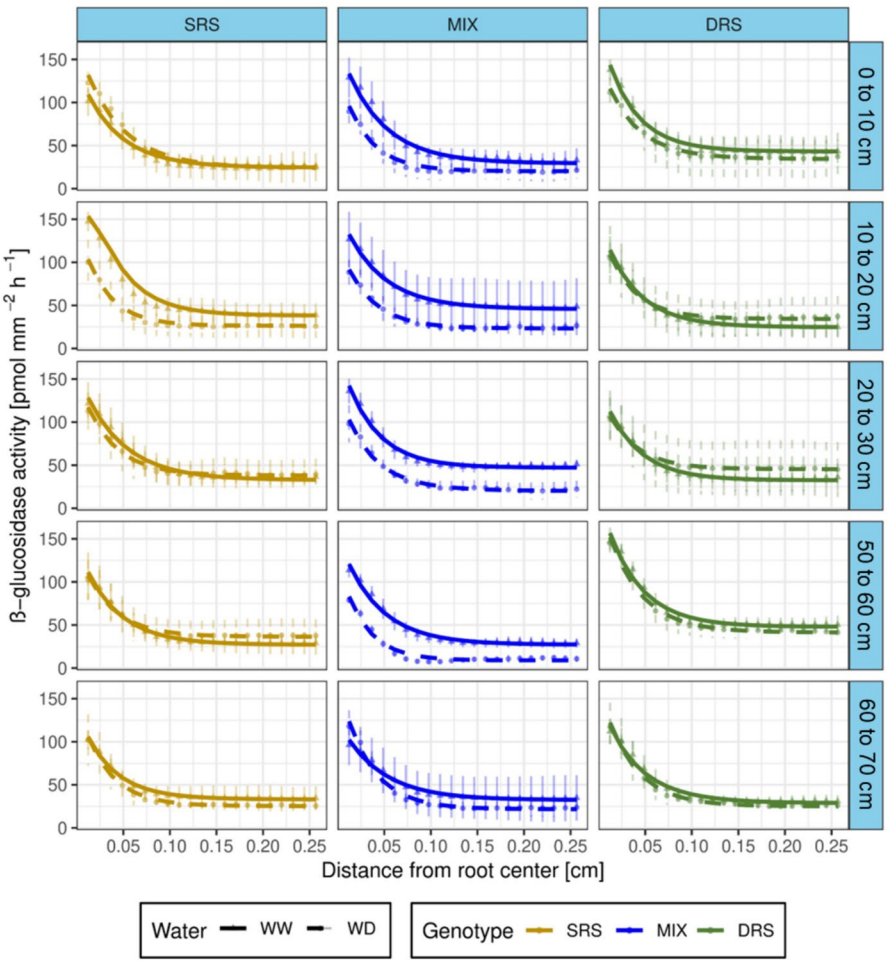

Fig. 10 Profile of the β-glucosidase gradient within the rhizosphere towards the surrounding soil for the shallow root system (SRS) (yellow), the mixture (MIX) (blue) and the deep root system (DRS) (green) at various soil depths under well-watered (WW) and water-deficit (WD) conditions. Dots represent mean BG activity. Lines represent the fit of an exponential decay function to mean enzyme activity profiles estimated from image analysis of zymograms. Data represent means ± standard deviation of three replicates, conducted across three runs. For each replicate the average BG activity was measured on 3 roots

Heuermann et al. (2019) showed in their experiment on interspecific competition among catch crops that root biomass is an important factor in N uptake from soil. In our experiment, the extracted root biomass was not significantly different between genotypes or water regimes. MRI data, however, revealed distinct root distribution patterns under well-watered conditions: SRS had significantly more root biomass in the topsoil (3–15 cm), while DRS displayed significantly higher root biomass in the subsoil (70–80 cm). Since MRI detects roots > 350 µm, the data particularly highlights changes in the larger root fractions, which play a crucial role in soil exploration, anchoring of the plant and in accessing deeper soil layers. Although fine roots, which are critical for nutrient and water uptake (Jackson et al. 1997) and make up a large proportion of the total root length of wheat (Moran et al. 2000), were not detected by MRI, our results underscore differences in how the two genotypes explored the soil columns with their root systems. Under water-deficit conditions, roots shrink in the upper layers as they lose water due to exchange with dry soil, reducing root water mass and, consequently, the MRI signal. This likely explains the lower signal in water-deficit versus well-watered treatments. Unlike aboveground biomass, root biomass of individual genotypes in mixtures could not be separated, preventing direct comparison of their root distribution in mixture versus monoculture. Nonetheless, results by Le Gall et al. (in press) showed that the SRS exhibited a higher root length density (RLD) in the topsoil (0–15 cm), whereas the DRS developed greater RLD in deeper soil layers (50–73 cm), reflecting their distinct rooting strategies. However, root growth is known to be influenced by the presence of roots from neighbouring plants (Morris et al. 2017),

which might explain why the distribution of roots in the soil within the mixture differed from what might be expected based on the monocultures. Contrary to our expectations, root biomass in the mixture was not at an intermediate level between the DRS and SRS in monoculture, as suggested by both the MRI data and the manually extracted root measurements. Li et al. (2006) also showed that when wheat and maize were grown together, wheat increased its root length density and rooted deeper soil layers more intensely than when grown in monoculture. Other studies found that this root response mainly results from a depletion of resources rather than the presence of neighbouring plants (Nord et al. 2011).

Release of assimilated carbon

Plant-plant interactions could also explain the observed C allocation into the soil. The reduced release of plant-derived carbon into the soil by the mixture under water-deficit conditions, compared to both well-watered conditions and monocultures under drought, may have been driven by a combination of above- and belowground interactions. Increased light competition, such as shading of one genotype by the other, could have affected photosynthetic activity and thus altered carbon allocation to the soil. At the same time, the spatial separation of the main root zones between genotypes may have decreased the need for root exudation to access nutrients (Dakora and Phillips 2002; Guillermo and Dudley 2007). Under well-watered conditions, greater water availability may have led to a higher demand for nutrients compared to water-deficit conditions, due to enhanced nutrient uptake efficiency and greater microbial abundance in the soil. This increased microbial abundance could lead to both competition for nutrients between plants and soil microorganisms, and stimulation of microorganisms by plants to enhance microbial nutrient release (Kuzyakov and Xu 2013). Consequently, plants may need to release more root exudates to ensure sufficient nutrient acquisition.

One exception was the subsoil, where the mixture showed an increased $\delta^{13}C$ signal in both roots and soil, even under water-deficit conditions. Within the root system, photoassimilates are mainly transported to the fast-growing and metabolically active root tips (Pausch and Kuzyakov 2011), where they may be released as mucilage, root border cells, or root exudates (Driouich et al. 2013; Ropitaux et al. 2019; Sasse et al. 2018). This indicates that active root growth was mainly concentrated in the subsoil of MIX and DRS compared to SRS. These results demonstrated that transport and release of photoassimilates and thus the active area of root growth and potential nutrient acquisition strategies varied between the genotypes and water regimes, potentially affecting nutrient uptake as reflected by the ^{15}N results.

Nitrogen uptake by plants

The observed differences in $\delta^{15}N$ signals align well with earlier findings regarding the primary root zones of the two genotypes. The DRS in the mixture demonstrated a higher N uptake efficiency from deeper soil layers under water-deficit conditions, as indicated by the high $\delta^{15}N$ signals in the youngest leaves after subsoil labelling. This reflects the ability of the DRS to explore subsoil resources more efficiently and was likely supported by its enhanced root exudation activity in these layers, aligning with the"steep, cheap, and deep"ideotype (Van der Bom et al. 2020). Le Gall et al. (in press) additionally observed increased root water uptake (RWU) from the subsoil by the DRS in monoculture and mixture under water-deficit conditions, also aligning well with our findings, suggesting that greater uptake of soil resources (N and water) is likely driven by more active roots at this specific soil depth. In contrast, the SRS in the mixture appeared less efficient in nutrient acquisition from deeper soil layers, possibly due to stronger competition with the DRS. However, following topsoil labelling, the $\delta^{15}N$ signals in the youngest leaves of the SRS increased, suggesting that under water-deficit conditions, the SRS focuses predominantly on nutrient (and water) uptake from the topsoil (Le Gall et al. in press), consistent with the"topsoil foraging"ideotype (Van der Bom et al. 2020). These findings underscore the complementary nutrient acquisition strategies of the two genotypes in mixture, with each adapting its resource-use pattern based on its root traits and ecological niche. This spatial niche differentiation implies that the combination of root-contrasting genotypes in mixture may also help reduce nutrient leaching, particularly nitrate, by enhancing nutrient capture across soil depths. We also found that there were no major differences in N uptake between the monocultures of DRS

and SRS after subsoil labelling, while greater differences were observed after topsoil labelling, indicating that the advantage of the DRS in nutrient uptake from deeper soil layers is smaller than that of the SRS from topsoil. Overall, the SRS in mono- and especially in mixed cultures appeared more efficient at N uptake compared to the DRS as indicated by its higher ^{15}N signal in the pooled leaf and stem and youngest fully developed leaf samples.

Microbial community and ^{13}C incorporation

The effect of high C allocation into the very subsoil by the mixture under water-deficit conditions correlated well with the abundances of fungi and gram-negative bacteria, which dominate the rhizosphere and rely on fresh C input from root exudates (Fierer et al. 2003; Kennedy and de Luna 2005). In the upper soil layers, on the other hand, the reduced allocation of photoassimilated C resulted in a smaller microbial community, as reflected by the lower abundance of bacterial and fungal PLFAs. This effect was especially pronounced for gram-negative bacteria, which rely more strongly than gram-positive bacteria on the availability of labile C (Fanin et al. 2019); hence, lower C input into the upper soil layers might have limited their abundance. These findings suggest that, due to the limited release of plant-derived carbon under water-deficit conditions, the expected synergistic effects of combining genotypes with contrasting root phenotypes in the mixture may not have resulted in improved plant–microbe interactions.

Conversely, under well-watered conditions, the incorporation of plant-derived C into the PLFAs of gram-positive and gram-negative bacteria and fungi was higher for the SRS in top- and subsoil compared to the DRS and MIX. The increased incorporation of plant-derived C into microbial PLFAs and NLFAs of the SRS suggests stronger nutrient competition between plants, which could enhance root exudation and thereby promote ^{13}C uptake by specific microbial groups. Regardless of the water content, fungi incorporated a high level of plant-derived C. The high $\delta^{13}C$ signal in the saprotrophic fungal PLFA (18:2ω6,9) compared to bacterial PLFAs is consistent with the results of Williams et al. (2006) and Müller et al. (2016) who found high incorporation of plant-derived C into the fungal PLFA 18:2ω6,9, indicating that fungi are a key group involved in the uptake of plant-derived C sources in soil. As fungi can actively grow towards soil resources due to their hyphal system (De Boer et al. 2005) and break down labile and complex organic substances (Ballhausen and de Boer 2016; Boberg et al. 2011; De Vries and Caruso 2016), they are more competitive in taking up resources from the rhizosphere of freshly formed, highly exudating root zones as compared to bacteria. Hannula et al. (2012) also showed that recently deposited plant C was utilised by saprotrophic fungi rather than arbuscular mycorrhizal fungi (AMF), which is consistent with our observation of a higher $\delta^{13}C$ signal in the saprotrophic fungal PLFAs than in the $NLFA_{AMF}$.

The trend towards lower abundance of $NLFA_{AMF}$ in the mixture compared to the monocultures under water-deficit conditions could also be related to less transport of photoassimilates into the roots and soil as indicated by the lower $\delta^{13}C$ signal in soil in the mixture. Arbuscular mycorrhizal fungi are particularly dependent on photosynthetically produced C compounds provided by the host plants, for which the host plant in turn receives nutrients such as N and phosphorus (Beslemes et al. 2023). Consequently, a reduction in the allocation of these compounds can result in lower abundance of AMFs. AMF further increase their host plants' drought tolerance due to their extraradical hyphae which aid in acquiring water from small soil pores inaccessible to plant roots (Chai and Schachtman 2022). Their abundance is therefore important in mitigating the effects of water stress on the plants (Begum et al. 2021; Das et al. 2021; Liu et al. 2020). Duan et al. (2024) observed that inoculation of wheat with AMF under water-deficit conditions leads to a higher plant productivity due to improved nutrient and water uptake, resulting in an up to 28.5% higher grain yield. The trend towards higher abundance of AMF in the upper soil layers of the WD-DRS and in the very topsoil of WD-SRS, could therefore improve not only nutrient but also water uptake. The higher abundance of the $NLFA_{AMF}$ combined with its increased $\delta^{13}C$ signal in the very topsoil of SRS under both water regimes, suggests that this root system primarily focuses on water and nutrient uptake from the topsoil. In contrast, under water-deficit conditions, the DRS appears to rely on symbiosis with AMF even in deeper soil layers in order to increase its water and nutrient uptake.

Microbial activity in the rhizosphere

The lower exudation/rhizodeposition of the mixture under water-deficit conditions was also reflected in reduced bulk BG activity and fewer areas with very high enzymatic activity. This was most likely due to reduced substrate availability (Hosseini et al. 2024), which in turn led to the observed formation of a smaller microbial community and thereby to lower BG production and hence activity (Taylor et al. 2002). Hosseini et al. (2024) concluded that the formation of microbial hotspots are fundamental traits for the development of future drought-resistant wheat genotypes. Since enzymatic hotspots, which are mainly located directly on or in close proximity to the roots (Hao et al. 2022; Sanaullah et al. 2016), play a key role in plant–microbe interactions, they are crucial to nutrient acquisition by both plants and microorganisms (Kuzyakov and Blagodatskaya 2015). Especially BG, which is considered the rate limiting enzyme in cellulose degradation, has an important function in providing glucose, used as an energy source by plants and microorganisms under drought stress (Hosseini et al. 2024). Exogenous application of small amounts of sugars have been found to facilitate the photosynthesis, seed germination, flowering, and senescence of plants under drought stress (Sami et al. 2016). Therefore, the lower BG activity observed for the mixture of the two genotypes used might negatively impact their yield quality and quantity (Lupwayi et al. 2015; Sainju et al. 2022).

A closer look at the BG gradient around the roots demonstrated that lower allocation of plant-derived C led to significantly lower BG activity near the root centre (E_0) and in bulk soil (E_{bulk}) of the WD-MIX compared to WW-MIX and the monocultures under both water regimes. The observed lower BG activity could indicate less colonization of active microorganisms near the root surface and within the surrounding soil under water-deficit conditions (Taylor et al. 2002). At 60–70 cm soil depth, the WD-MIX, however, had a BG gradient similar to the WW-MIX due to greater C allocation into this specific soil layer. Root exudation as an important driver of enzymatic activity in the rhizosphere is controlled not only by the plant species and developmental stage, but also by root morphology (Bilyera et al. 2021; Kuzyakov and Razavi et al. 2019; Zhang et al. 2019). Root tips and lateral root emergence sites have especially high levels of root exudation (Van Egeraat 1975). This occurs because the growth of lateral roots damages the primary root cell cortex (Neumann and Römheld 2002). Additionally, young root tips have not yet formed cell walls, leading to leakage of labile organic C sources from the roots (McCully and Canny 1985). The differences in root exudation of the mixture between both water regimes might therefore also be caused by differences in root morphology indicating the formation of smaller amounts of lateral roots and root tips in the mixture under water-deficit conditions. The reduced formation of lateral roots, which typically show an improved growth when nutrients are scarce (Morgan and Connolly et al. 2013), may indicate that nutrient supply to the plant was sufficient even under water-deficit conditions. This could be caused by a lower competition for nutrients between genotypes with contrasting main rooting zones. Increased exudation of photoassimilated C into the soil of the monocultures and the WW-MIX might therefore have resulted from stronger competition for nutrients. In monocultures, this competition could result from similar main rooting zones. In mixtures under well-watered conditions, increased plant performance due to better water supply raises the plants nutrient requirements therefore possibly increasing lateral root formation. Observed BG gradients around the roots suggest that enzymatic activity in the soil was not solely dependent on root biomass, but also on root morphological characteristics.

Conclusion

This study provides insights into how combining wheat genotypes with contrasting root phenotypes influences microbial dynamics and nutrient uptake under different water regimes. Combining root contrasting wheat genotypes reduced microbial activity, exudation and enzyme function under water deficit conditions while complementarity in nutrient acquisition strategies. While these findings highlight the potential for combining genotypes with contrasting root phenotypes to optimize nutrient use, it is important to note that yield, a critical factor for agricultural application, was not assessed due to the restricted incubation time, to avoid artificial effects caused by the limited soil volume in the columns. Furthermore, since only one genotype per

root type was used, genotype-specific effects cannot be excluded, and the results are not necessarily attributable solely to differences in root architecture. Future field experiments covering the entire growth period and involving different genotypes that develop either a deep or a shallow root system are therefore needed to evaluate whether these interactions translate into higher or more stable yields in water-limited systems. Such research could offer practical strategies for designing crop systems to improve resource use efficiency and promote resilience of agro-ecosystems.

Acknowledgements The authors thank Sabine Rudolph, Heike Haslwimmer, Chao Gao, Ahmet Sircan, Laura Lutz, Berenike Breuer, Vinzent Leyrer, and Philipp Mäder for their assistance during the experimental setup and lab work and Kathleen Regan for English corrections. We gladly acknowledge the help of Fabian Isensee and Lars Krämer from the Helmholtz imaging support hub who developed the MRI root segmentation neural network. We also thank the German Federal Ministry of Education and Research (BMBF) for funding.

Authors contributions Adrian Lattacher, Samuel Le Gall, Youri Rothfuss, Moritz Harings, Ellen Kandeler and Christian Poll contributed to the conception and design of the study. Samir Alahmad and Lee Hickey developed and provided the required wheat lines. Samuel Le Gall, Moritz Harings, Youri Rothfuss, Dagmar van Dusschoten and Adrian Lattacher conducted the column experiment in the climate chamber. Wolfgang Armbruster conducted the isotope analysis. Adrian Lattacher performed the sample analysis. Samuel Le Gall and Daniel Pflugfelder provided data on the MRI scans of the root system. Adrian Lattacher conducted the data evaluation and statistics. The first draft of the manuscript was written by Adrian Lattacher under supervision of Ellen Kandeler and Christian Poll. All authors commented on previous versions of the manuscript. All authors read and approved the final manuscript.

Funding Open Access funding enabled and organized by Projekt DEAL. This paper was written within the context of the phase I of the CROP project (Combining ROot contrasted Phenotypes for more resilient agro-ecosystem) (project number: FKZ 031B0909A), which is founded by the German Federal Ministry of Education and Research (BMBF). The experimental wheat lines examined in this study were developed through the Grains Research and Development Corporation (GRDC) "Rooty" project (ID 9176855), which formed part of the International Wheat Yield Partnership Consortium (IWYP122).

Data availability The datasets generated during this study are available from the corresponding author on request.

Code availability This is not applicable to the manuscript.

Declarations

Competing interests The authors have no relevant financial or non-financial interests to disclose.

References

Abramoff MD, Magalhaes PJ, Ram SJ (2004) Image processing with Image. J Biophonics Int 11(7):36–42

Alahmad S, El Hassouni K, Bassi FM, Dinglasan E, Youssef C, Quarry G, Aksoy A, Mazzucotelli E, Juhász A, Able JA, Christopher J, Voss-Fels KP, Hickey LT (2019) A major root architecture QTL responding to water limitation in durum wheat. Front Plant Sci 10:436

Ballhausen MB, de Boer W (2016) The sapro-rhizosphere: carbon flow from saprotrophic fungi into fungus-feeding bacteria. Soil Biol Biochem 102:14–17

Bardgett RD, Hobbs PJ, Frostegård Å (1996) Changes in soil fungal:bacterial biomass ratios following reductions in the intensity of management of an upland grass-land. Biol Fertil Soils 22:261–264

Bécu T, Barot S, Lata JC, Roux XL, Enjalbert J, Niboyet A (2024) Increasing intraspecific diversity of wheat affects plant nutrient contents but not N recovery in the plant-soil system. Basic Appl Ecol 74:24–34

Begum N, Akhtar K, Ahanger MA, Iqbal M, Wang P, Nabil S, Mustafa NS, Zhang L (2021) Arbuscular mycorrhizal fungi improve growth, essential oil, secondary metabolism, and yield of tobacco (*Nicotiana tabacum* L.) under drought stress conditions. Environ Sci Pollut Res 28:4576–45295

Beslemes D, Tigka E, Roussis I, Kakabouki I, Mavroeidis A, Vlachostergios D (2023) Effect of arbuscular mycorrhizal fungi on nitrogen and phosphorus uptake efficiency and crop productivity of two-rowed barley under different crop production systems. Plants 12:1908

Beule L, Guerra V, Lehtsaar E, Vaupel A (2022) Digging deeper: microbial communities in subsoil are strongly

promoted by trees in temperate agroforestry systems. Plant Soil 480:423–437
Bilyera N, Zhang X, Duddek P, Fan L, Banfield CC, Schlüter S, Carminati A, Kaestner A, Ahmed MA, Kuzyakov Y, Dippold MA, Spielvogel S, Razavi BS (2021) Maize genotype-specific exudation strategies: An adaptive mechanism to increase microbial activity in the rhizosphere. Soil Biol Biochem 162:108426
Bligh EG, Dyer WJ (1959) A rapid method of total lipid extraction and purification. Can J Biochem Physiol 37:911–917
Boberg JB, Nasholm T, Finlay RD, Stenlid J, Lindahl BD (2011) Nitrogen availability affects saprotrophic basidiomycetes decomposing pine needles in a long term laboratory study. Fungal Ecol 4(6):408–416
Cai G, Vanderborght J, Klotzsche A, Van Der Kruk J, Neumann J, Hermes N, Vereecken H (2016) Construction of minirhizotron facilities for investigating root zone processes. Vadose Zone J 15:1–13
Cantarel AAM, Allard V, Andrieu B, Barot S, Enjalbert J, Gervaix J, Goldringer I, Pommier T, Saint-Jean S, Le Roux X (2021) Journal of Experimental Botany 7284:1166–1180
Chai YN, Schachtmann DP (2022) Root exudates impact plant performance under abiotic stress. Trends Plant Sci 27:80–91
Colombo M, Roumet P, Salon C, Jeudy C, Lamboeuf M, Lafarge S, Dumas AV, Dubreuil P, Ngo W, Derepas B, Beauchêne K, Allard V, Gouis J, Rincent R (2022) Genetic analysis of platform-phenotyped root system architecture of bread and durum wheat in relation to agronomic traits. Front Plant Sci 13:853601
Dakora FD, Phillips DA (2002) Root exudates as mediators of mineral acquisition in low-nutrient environments. Plant Soil 245:35–47
Das D, Basar NU, Ullah H, Salin KP, Datta A (2021) Interactive effect of silicon and mycorrhizal inoculation on growth, yield and water productivity of rice under water-deficit stress. J Plant Nutr 44(18):2756–2769
De Vries FT, Caruso T (2016) Eating from the same plate? Revisiting the role of labile carbon inputs in the soil food web. Soil Biol Biochem 102:4–9
De Boer W, Folman LB, Summerbell RC, Boddy L (2005) Living in a fungal world: impact of fungi on soil bacterial niche development. FEMS Microbiol Rev 29(4):795–811
Driouich A, Follet-Gueye ML, Gibouin MV, Hawes M (2013) Root border cells and secretions as critical elements in plant host defense. Curr Opin Plant Biol 16:489–495
Duan HX, Luo CL, Zhou R, Zhao L, Zhu SG, Chen Y, Zhu Y, Xiong YC (2024) AM fungus promotes wheat grain filling via improving rhizospheric water & nutrient availability under drought and low density. Appl Soil Ecol 193:105159
Dunbabin V, Diggle A, Rengel Z (2003) Is there an optimal root architecture for nitrate capture in leaching environments? Plant, Cell Environ 26:835–844
Fanin N, Kardol P, Farrell M, Nilsson MC, Gundale MJ, Wardle DA (2019) The ratio of gram-positive to gram-negative bacterial PLFA markers as an indicator of carbon availability in organic soils. Soil Biol Biochem 128:111–114
Federle TW (1986) Microbial distribution in soil-new techniques. In: Megusar F, Gantar M (eds) Perspectives in microbial ecology. Slovene Society for Microbiology, Ljubljana, pp 493–498
Fierer N, Schimel JP, Holden PA (2003) Variations in microbial community composition through two soil depth profiles. Soil Biol Biochem 35:167–176
Fox J, Weisberg S (2019) An R Companion to Applied Regression, Third edition. Sage, Thousand Oaks CA. https://socialsciences.mcmaster.ca/jfox/Books/Companion/
Frostegård Å, Tunlid A, Bååth E (1991) Microbial biomass measured as total lipid phosphate in soils of different organic content. J Microbial Methods 14:151–163
Gaba S, Lescourret F, Boudsocq S, Enjalbert J, Hinsinger P, Journet EP, Navas ML, Wery J, Louarn G, Malézieux E, Pelzer E, Prudent M, Ozier-Lafontaine H (2014) Multiple cropping systems as drivers for providing multiple ecosystem services: from concepts to design. Agron Sustain Dev 35(2):607–623
Galindo-Castañeda T, Lynch JP, Six J, Hartmann M (2022) Improving soil resource uptake by plants through capitalizing on synergies between root architecture and anatomy and root-associated microorganisms. Front Plant Sci 13:827369
Galindo-Castañeda T, Hartmann M, Lynch JP (2024) Location: root architecture structures rhizosphere microbial associations. J Exp Bot 75:594–604
Le Gall S, Van Duschotten D, Lattacher A, Giraud M, Harings M, Deseano Diaz P, Pflugfelder D, Alahmad S, Hickey LT, Sircan A, Kandeler E, Lobet G, Pagel H, Poll C, Schnepf A, Vereecken H, Javaux M, Rothfuss Y (in press) Combining root-contrasted spring wheat phenotypes for a better use of water resources in soil? Evidence from a column-scale water stable isotopic experiment. Plant and Soil
Gobran GR, Clegg S (1996) A conceptual model for nutrient availability in the mineral soil-root system. Can J Soil Sci 76:125–131
Guber A, Blagodatskaya E, Juyal A, Razavi BS, Kuzyakov Y, Kravchenko A (2021) Time-lapse approach to correct deficiencies of 2D soil zymography. Soil Biol Biochem 157:108225
Guillermo PM, Dudley SA (2007) Above- and below-ground competition cues elicit independent responses. British Ecological Society 95(2):261–272
Hannula SE, Boschker HTS, de Boer W, van Veen JA (2012) ^{13}C pulse-labeling assessment of the community structure of active fungi in the rhizosphere of a genetically starch-modified potato (Solanum tuberosum) cultivar and its parental isoline. New Phytol 194(3):784–799
Hao C, Dungait JAJ, Wie X, Ge T, Kuzyakov Y, Cui Z, Tian J, Zhang F (2022) Maize root exudate composition alters rhizosphere bacterial community to control hotspots of hydrolase activity in response to nitrogen supply. Soil Biol Biochem 170:108717
Heitkötter J, Marschner B (2018) Is there anybody out there? Substrate availability controls microbial activity outside of hotspots in subsoils. Soil Systems 2:35
Heuermann D, Gentsch N, Boy J, Schweneker D, Feuerstein U, Groß J, bauer B, Guggenberger G, Wirén (2019) Interspecific competition among catch crops modifies vertical

root biomass distribution and nitrate scavenging in soils. Sci Rep 9:11531
Hosseini SS, Razavi BS, Lakzian A (2024) Drought tolerance of wheat genotypes is associated with rhizosphere size and enzyme systems. Plant Soil. https://doi.org/10.1007/s11104-024-06576-z
Isbell F, Adler PR, Eisenhauer N, Fornara D, Kimmel K, Kremen C, Letourneau DK, Liebman M, Polley HW, Quijas S, Scherer-Lorenz M (2017) Benefits of increasing plant diversity in sustainable agroecosystems. J Ecol 105(4):871–879
Isensee F, Jaeger PF, Kohl SAA, Petersen J, Maier-Hein KH (2021) nnU-Net: a self-configurating method for deep learning-based biomedical image segmentation. Nat Methods 18:203–211. https://doi.org/10.1038/s41592-020-01008-z
Ivić M, Grljušić S, Plavšin S, Dvojković K, Lovrić A, Rajković B, Maričević M, Černe M, Popović B, Lončarić Z, Bentley AR, Swarbreck S, Šarčević H, Novoselović (2021) Variation for nitrogen use efficiency traits in wheat under contrasting nitrogen treatments in south-eastern europe. Front Plant Sci 12:682333
Jackson RB, Mooney HA, Schulze ED (1997) A global budget for fine root biomass, surface area, and nutrient contents. Ecology 94(14):7362–7366
Jamali H, Quayle WC, Baldock J (2015) reducing nitrous oxide emissions and nitrogen leaching losses from irrigated arable cropping in Australia trough optimized irrigation scheduling. Agric for Meteorol 208:32–39
Joergensen RG (1996) The fumigation-extraction method to estimate soil microbial biomass: calibration of the KEC value. Soil Biol Biochem 28:25–31
Joseph J, Luster J, Bottero A, Buser N, Baechli L, Sever K, Gessler A (2021) Effect of drought on nitrogen uptake and carbon dynamics in trees. Tree Physiol 41(6):927–943
Kandeler E (2015) Physiological and biochemical methods for studying soil biota and their functions. In: Paul EA (ed) Soil Microbiology, Ecology and Biochemistry, 4th edn. Academic Press, San Diego, pp 187–222
Kang Y, Rambla C, Haeften SV, Fu B, Akinlade O, Potgieter AB, Borrell AK, Mace E, Jordan DR, Alahmad S, Hickey LT (2024) Seminal root angle is associated with root system architecture in durum wheat. Food Energy Security 13:e570
Keiluweit M, Bougoure JJ, Nico PS, Pett-Ridge J, Weber PK, Kleber M (2015) Mineral protection of soil carbon counteracted by root exudates. Nat Clim Chang 5:588–595
Kennedy AC, de Luna LZ (2005) Rhizosphere. In: Hillel D (ed) Encyclopedia of soils in the environment. Elsevier, Oxford, pp 399–406
Kramer C, Gleixner G (2008) Soil organic matter in soil depth profiles: distinct carbon preferences of microbial groups during carbon transformation. Soil Biol Biochem 40:425–433
Kuzyakov Y, Blagodatskaya E (2015) Microbial hotspots and hot moments in soil: Concept & review. Soil Biol Biochem 83:184–199
Kuzyakov Y, Razavi BS (2019) Rhizosphere size and shape: temporal dynamics and spatial stationarity. Soil Biol Biochem 135:343–360
Kuzyakov Y, Xu X (2013) Competition between roots and microorganisms for nitrogen: mechanisms and ecological relevance. New Phytol 198:656–669
Langridge P, Braun H, Hulke B, Ober E, Prasanna BM (2021) Breeding crops for climate resilience. Theor Appl Genet 134:1607–1611
Lattacher A, Le Gall S, Rothfuss Y, Gao C, Harings M, Pagel H, Giraud M, Alahmad S, Hickey LT, Kandeler E, Poll C (2025) Rooting for microbes: impact of root architecture on the microbial community and function in top- and subsoil. Plant Soil. https://doi.org/10.1007/s11104-024-07181-w
Le Gall S, Lapie C, Cajot F, Doussan C, Corridor L, Bérard A (2024) Chemical diversity of crop root mucilages. implications for their maximal water content and decomposition. Rhizosphere 29:100858
Li L, Sun J, Zhang F, Guo T, Bao X, Smith FA, Smith SE (2006) Root distribution and interactions between intercropped species. Oecologia 147:280–290
Lichstein JW, Dushoff J, Levin SA, Pacala SW (2007) Intraspecific variation and species coexistence. Am Nat 170(6):807–818
Liste HH, White JC (2008) Plant hydraulic lift of soil water – implications for crop production and land restoration. Plant Soil 313:1–17
Liu CY, Wang YJ, Wu QS, Yang TY, Kuča K (2020) Arbuscular mycorrhizal fungi improve the antioxidant capacity of tea (*Camellia sinensis*) seedlings under drought stress. Notulae Botanicae Horti Agrobotanici Cluj-Napoca 48(4):1993–2005
Lupwayi NZ, Harker KN, O'Donovan JT, Turkington TK, Blackshaw RE, Hall LM, Willenborg CJ, Gan Y, Lafond GP, May WE, Grant CA (2015) Relating soil microbial properties to yields of no-till canola on the Canadian prairies. Eur J Agronomy 62:110–119
Ma W, Tang S, Dengzeng Z, Zhang D, Zhang T, Ma X (2022) Root exudates contribute to belowground ecosystem hotspots: a review. Front Microbiol 13:937940
Marhan S, Kandeler E, Rein S, Fangmeier A, Niklaus A (2010) Indirect effects of soil moisture reverse soil C sequestration responses of a spring wheat agroecosystem to elevated CO_2. Glob Chang Biol 16:469–483
McCully ME, Canny MJ (1985) Localisation of translocated ^{14}C in roots and root exudates of field-grown maize. Physiol Plant 65:380–392
Moran CJ, Pierret A, Stevenson AW (2000) X-ray absorption and phase contrast imaging to study the interplay between plant roots and soil structure. Plant Soil 223:99–115
Morgan JB, Connolly EL (2013) Plant-soil interactions: Nutrient uptake. Nat Educ Knowledge 4(8):2
Morris EC, Griffiths M, Golebiowska A, Mairhofer S, Burr-Hersey J, Goh T, von Wagenheim D, Atkinson B, Sturrock CJ, Lynch JP, Vissenberg K, Ritz K, Wells DM, Mooney SJ, Bennett J (2017) Shaping 3D root system architecture. Curr Biol 27:R919–R930
Müller K, Susanne K, Haslwimmer H, Marhan S, Scheunemann N, Butenschön O, Scheu S, Kandeler E (2016) carbon transfer from maize roots and litter into bacteria and fungi depends on soil depth and time. Soil Biol Biochem 93:79–89

Nakhforoosh A, Nagel KA, Fiorani F, Bodner G (2021) Deep soil exploration vs. topsoil exploitation: distinctive rooting strategies between wheat landraces and wild relatives. Plant Soil 459:397–421

Neumann G, Römheld V (2002) Root-induced changes in the availability of nutrients in the rhizosphere. In: Waisel Y, Eshel A, Beeckman T, Kafkafi U (eds) Plant roots: the hidden half, 3rd edn. Marcel Dekker Inc., New York, pp 617–649

Nord EA, Zhang CC, Lynch JP (2011) Root responses to neighbouring plants in common bean are mediated by nutrient concentration rather than self/non-self recognition. Funct Plant Biol 38:941–952

Ober ES, Alahmad S, Cockram J, Forestan C, Hickey LT, Kant J, Maccaferri M, Marr E, Milner M, Pinto F, Rambla C, Reynolds M, Salvi S, Sciara G, Snowdon RJ, Thomelin P, Tuberosa R, Uauy C, Voss-Fels WE, Watt M (2021) Wheat root systems as breeding target for climate resilience. Theor Appl Genet 134:1645–1662

Olsson PA, Francis R, Read DJ, Söderström B (1998) Growth of arbuscular mycorrhizal mycelium in calcareous dune sand and its interaction with other soil micro-organisms as estimated by measurement of specific fatty acids. Plant Soil 201:9–16

Østergård H, Finckh MR, Fontaine L, Goldringer I, Hoad SP, Kristensen K, Lammberts van Bueren ET, Mascher F, Munk L, Wolfe MS (2009) Time for a shift in crop production: embracing complexity through diversity at all levels. Perspective. J Sci Food Agric 89(9):1439–1445

Paez-Garcia A, Motes CM, Scheible WR, Chen R, Blancaflor EB, Monteros MJ (2015) Root traits and phenotyping strategies for plant improvement. Plants 4:334–355

Pausch J, Kuzyakov Y (2011) Photoassimilate allocation and dynamics of hotspots in roots visualized by ^{14}C phosphor imaging. J Plant Nutr Soil Sci 174:12–19

Pinheiro JC, Bates DM (2000) Mixed-effects models in S and S-PLUS. Springer, New York. https://doi.org/10.1007/b98882

Preusser S, Liebmann P, Stucke A, Wirsching J, Müller K, Mikutta R, Guggenberger G, Don A, Kalbitz K, Bachmann J, Marhan S, Poll C, Kandeler E (2021) Microbial utilisation of aboveground litter-derived organic carbon within a sandy dystric cambisol profile. Frontiers in Soil Science 1:666950

Prieto I, Armas C, Pugnaire FI (2012) Water release trough plant roots: new insights into its consequence at the plant and ecosystem level. New Phytol 193:830–841

R Core Team (2020) R: A Language and environment for statistical computing. R Foundation for Statistical Computing, Vienna, Austria. URL: https://www.R-project.org/

Rambla C, Van Der Meer S, Voss-Fels KP, Makhoul M, Obermeier C, Snowdon R, Ober ES, Watt M, Alahmad S, Hickey LT (2022) A toolkit to rapidly modify root systems through single plant selection. Plant Methods 18:1–13

Razavi BS, Zarebanadkouki M, Blagodatskaya E, Kuzyakov Y (2016) Rhizosphere shape of lentil and maize: spatial distribution of enzyme activities. Soil Biol Biochem 96:229–237

Ropitaux M, Bernard S, Follet-Gueye ML, Vicré M, Boulogne I, Driouich A (2019) Xyloglucan and cellulose form molecular cross-bridges connecting root border cells in pea (Pisum sativum). Plant Physiol Biochem 139:191–196

Sainju UM, Liptzin D, Dangi SM (2022) Enzyme activities as soil health indicators in relation to soil characteristics and crop production. Agrosyst, Geosci Environ 5(3):20297

Sami F, Yusuf M, Faizan M, Faraz A, Hayat S (2016) Role of sugars under abiotic stress. Plant Physiol Biochem 109:54–61

Sanaullah M, Razavi BS, Blagodatskaya E, Kuzyakov Y (2016) Spatial distribution and catalytic mechanisms of β-glucosidase activity at the root-soil interface. Biol Fertil Soils 52:505–514

Sasse J, Martinoia E, Northen T (2018) Feed your friends: Do plant exudates shape the root microbiome? Trends Plant Sci 23:25–41

Tadesse W, Sanchez-Garcia M, Assefa SG, Amri A, Bishaw Z, Ogbonnaya FC, Baum M (2019) Genetic gains in wheat breeding and its role in feeding the world. Crop Breeding, Genet Genom 1:e190005

Taylor JP, Wilson B, Mills MS, Burns RG (2002) Comparison of microbial numbers and enzymatic activities in surface soils and subsoils using various techniques. Soil Biol Biochem 34(3):387–401

Van der Bom FJT, Williams A, Bell MJ (2020) Root architecture for improved resource capture: trade-offs in complex environments. J Exp Bot 71:5752–5763

Van Egeraat AWSM (1975) Exudation of ninhydrin-positive compounds by pea-seedling roots: a study of the sites of exudation and of the composition of the exudate. Plant Soil 42:37–47

Van Dusschoten D, Metzner R, Kochs J, Postma JA, Pflugfelder D, Brühl J, Schurr U, Jahnke S (2016) Quantitative 3D analysis of plant roots growing in soil using magnetic resonance imaging. Plant Physiol 170:1176–1188

Vance ED, Brookes PC, Jenkinson DS (1987) An extraction method for measuring soil microbial biomass C. Soil Biol Biochem 19:703–707

Voss-Fels KP, Snowdon RJ, Hickey LT (2018) Designer roots for future crops. Trends Plant Sci 23:957–960

Weihermüller L, Huisman JA, Lambot S, Herbst M, Vereecken H (2007) Mapping the spatial variation of soil water content at the field scale with different ground penetrating radar techniques. J Hydrol 340:205–216

Wen T, Yu GH, Hong WD, Yuan J, Niu GQ, Xie PH, Sun FS, Guo LD, Kuzyakov Y, Shen QR (2022) Root exudate chemistry affects soil carbon mobilization via microbial community reassembly. Fundam Res 2:697–707

Williams MA, Myrold DD, Bottomley PJ (2006) Carbon flow from ^{13}C-labeled straw and root residues into the phospholipid fatty acids of a soil microbial community under field conditions. Soil Biol Biochem 38(4):759–768

Yuan X, Wang Y, Ji P, Wu P, Sheffield J, Otkin JA (2023) A global transition to flash droughts under climate change. Science 380:187–191

Zhang X, Dippold MA, Kuzyakov Y, Razavi BS (2019) Spatial patterns of enzyme activities depends on root exudate composition. Soil Biol Biochem 133:83–93